Amina BAGDAOUI[1], Amina BENDAOUDI[1], Ali JAFFARI[2]
Laboratory of Electromagnetic, Photonics and Optoelectronics
University of Sidi Bel Abbes, Algeria (1). CNRS, France (2).

doi:10.15199/48.2024.04.07

Intensity Only Multi-Materials Image Reconstruction

Abstract. *The phase retrieval problem is a challenging issue in image processing, which aims to reconstruct an object from magnitude-only measurements in the Fourier domain. Most methods for phase retrieval are deterministic frameworks, and their results are often unsatisfactory when the available measured spectrum magnitude is corrupted by additive noise. The a priori knowledge characterizing the object is the finite number of homogeneous materials that compose it. This knowledge is represented by a Gauss-Markov prior. Iterative joint reconstruction and classification techniques are used to calculate a satisfactory reconstruction. The reconstructed image is obtained by first specifying the a posteriori distributions of all the unknowns, followed by the application of the Gibbs sampling algorithm to estimate the posterior mean of the unknowns. Simulation results are presented to demonstrate the accuracy of the proposed prior compared to the case where only the Potts-Markov prior is used.*

Streszczenie. *Problem odzyskiwania fazy stanowi wyzwanie w przetwarzaniu obrazu, którego celem jest rekonstrukcja obiektu na podstawie pomiarów wielkości w domenie Fouriera. Większość metod odzyskiwania fazy to metody deterministyczne, a ich wyniki są często niezadowalające, gdy wielkość dostępnego zmierzonego widma jest zniekształcona przez szum addytywny. Wiedzą aprioryczną charakteryzującą obiekt jest skończona liczba jednorodnych materiałów, które go tworzą. Wiedzę tę reprezentuje przeor Gaussa-Markowa. Aby obliczyć zadowalającą rekonstrukcję, stosuje się iteracyjne techniki rekonstrukcji i klasyfikacji stawów. Zrekonstruowany obraz uzyskuje się poprzez określenie rozkładów a posteriori wszystkich niewiadomych, a następnie zastosowanie algorytmu próbkowania Gibbsa do oszacowania średniej późniejszej niewiadomych. Wyniki symulacji przedstawiono w celu wykazania dokładności proponowanego stanu pierwotnego w porównaniu z przypadkiem, w którym używany jest tylko stan Pottsa-Markowa****(Rekonstrukcja obrazu z wielu materiałów, tylko intensywność)***

Keywords: Phase retrieval, Fourier Synthesis (FS), Inverse Problems, Bayesian estimation, Hidden Markov, Markov Chain Monte Carlo (MCMC)
Słowa kluczowe: Odzyskiwanie faz, synteza Fouriera (FS), problemy odwrotne, estymacja bayesowska, ukryty Markow, łańcuch Markowa Monte Carlo (MCMC)

Introduction

For many years, the phase retrieval problem, which involves reconstructing an object solely from its spectral magnitude in the Fourier domain, has been a significant and long-standing challenge. Several optical detection techniques, including coherent diffraction imaging (CDI), face the challenge of not being able to directly measure the phase of a light wave. In Figure.1, it is illustrated that the sensors used in these techniques only record the magnitude of diffracted rays while losing the phase information. However, the phase is essential for inverting the 2D Fourier transform and reconstructing the image accurately. This problem arises in various applications including X-ray crystallography [1], [2], [3], diffraction imaging [4], [9], acoustics [10], optics [11], [12], astronomy [13], and quantum mechanics [14]. The primary objective of this task is to determine a method for retrieving the missing phase information from the measurements, which is challenging to obtain. The ultimate goal is to recover the unknown object using only the intensity of the measurements (spectrum magnitude).

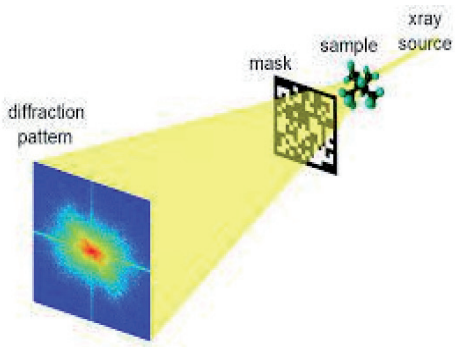

Fig. 1: A typical setup for phase retrieval in diffraction imaging.

In this paper the aim of the image reconstruction task is to recover the original image denoted as $f(\mathbf{r})$, where $\mathbf{r} \in \mathbf{R}^2$ from the noisy magnitude of its Fourier transform represented as $g(\omega)$, where $\omega \in \mathbf{R}^2$. The reconstruction process relies on the known a priori information about the image. The mathematical modeling of this imaging phenomenon is described by the following equation:

$$\begin{aligned} g(\omega) &= G(F(\omega)) + \epsilon(\omega) \\ F(\omega) &= \int f(\mathbf{r}) e^{-j\omega^T \mathbf{r}} d\mathbf{r} \quad , \quad G(.) = |.| \end{aligned} \tag{1}$$

Over the past four decades, several phase retrieval algorithms have been proposed. One of the earliest and well-known methods is the Gerchberg-Saxton algorithm [15] which involves alternating projections and iteratively updating the unknown phases of the measurements and the unknown signals in both spatial and frequency domains. Another approach is the alternating minimization technique with spectrum initialization [16]. In recent years, a convex relaxation-based method called PhaseLift has been introduced for phase retrieval [17]. PhaseLift aims to recover the phase from intensity measurements by incorporating structured illuminations and leveraging ideas from convex programming. It solves a convex optimization problem inspired by the matrix completion literature, enabling the recovery of a complex-valued object from the magnitude of only a few diffracted patterns. However, it should be noted that applying PhaseLift results in lifting the signal of interest to a high-dimensional space, which increases the computational complexity of the phase lift. To avoid this drawback, non-convex phase retrieval algorithms that work directly on the original signal space, such as the alternating minimization algorithm, have been developed [16]. The Wirtinger method [18] and its variants [19], as well as PhaseMax [20], were proposed as approaches that utilize semi-definite relaxation to elevate the phase retrieval problem to a higher dimension. In this paper, we employ a Bayesian approach to quantitatively reconstruct homogeneous multi-material image from their spectral magnitude measurements in the Fourier domain, even in the presence of incomplete data. The proposed method in our study utilizes a non-linear frequency domain observation model.

Specifically, we employ a Bayesian approach with a stochastic framework. It is important to note that if we assume an image with $\mathbf{r}$ pixels in the spatial domain belongs to a finite lattice $\mathbf{R}$, the lattice will consist of $\mathbf{n}$ pixels. We consider a discrete lattice with a length of $\mathbf{N}$. In the subsequent equations, vector notation will be employed. The approach introduce a Bayesian framework to handle a priori models for the pixel distribution of the desired image results. It is founded on the assumption that the reconstructed image consists of homogeneous materials. Consequently, the a priori probability distribution of the pixels is modeled using a Finite Mixture Model (FMM) [23], enabling classification into a finite number of classes through a Potts Markov Model (PMM) [24] for labels. The Potts Markov Random Field (MRF) is utilized to model the spatial relationships and dependencies between neighboring pixels. It promotes smoothness and encourages similarity between adjacent pixels within the same class.

$$\mathbf{g} = \mathbf{H}(\mathbf{f}) + \epsilon \tag{2}$$

where $\mathbf{g} = \{g(\omega), \omega \in \Omega\}$ represent the observed values, $\mathbf{f} = \{f(\mathbf{r}), \mathbf{r} \in R\}$ denotes the original image, $\mathbf{H} : R^n \longrightarrow R_+^N$ refers to the truncation of the magnitude Fourier transform of the image $\mathbf{f}$, and ϵ represents the measurement noise.

Additionally, a new Gauss-Markov a priori model is introduced to capture pixel dependencies within each class specifically. This model assumes that the pixel values within a class follow a Gaussian distribution, and the dependencies between pixels within the same class are described by a Markov property. This enables the model to capture fine-grained details and dependencies within individual classes while maintaining the global spatial coherence imposed by the Potts MRF. The combination of the FMM, Potts MRF, and Gauss-Markov a priori model provides a comprehensive framework for capturing both global and local characteristics of the image, allowing for more accurate and realistic pixel distributions and dependencies within the image. The effectiveness and accuracy of the proposed framework can be demonstrated, showing its ability to achieve high-quality reconstructions and preserve the characteristics of the original image.

The structure of the paper is as follows: Section 2: Fundamentals of the Bayesian estimation framework for images. Section 3: Description of the a priori model for image pixel distribution, which consists of a Finite Mixture Model (FMM) and a Potts Markov Random Field (MRF) and a new a Gauss-Markov a priori model for pixel dependency in each class Section 4: Expression of the necessary posterior laws to implement the Quasi-Monte Carlo Markov Chain (QMCMC) Gibbs sampling. Section 5: QMCMC Gibbs sampling algorithm is presented. The results of reconstructed are presented first in Section 6 when the number of constituent materials (number of classes) is known. The algorithm is tested in various case iterations. A comparison study is presented between our approach and three phase retrieval algorithms, including the iterative phase retrieval in coherent diffractive imaging method. [6], which is largely based on the error reduction iterative phase retrieval algorithm described by Fienup [5],The second algorithm is largely based on Fienup's method [5], with the inclusion of amplitude constraints in the object domain. The phase retrieval framework includes a second comparison between Potts-Markov priors and Gauss-Markov priors. Conclusions and the perspective regarding this work are provided in Section 7.

Bayesian estimation for image reconstruction

- Utilize the forward model (Eq. 2) and make certain assumptions about the noise to derive the likelihood $p(g/f, \theta)$, where θ represents the parameters of the noise probability distribution.
- Utilize all the prior information or the desired properties for the solution to assign an a priori probability distribution $p(f, \theta)$ where θ is its parameter.
- Utilize the Bayesian approach to derive:
  1. the a posteriori probability distribution
  $$p(\mathbf{f}|\mathbf{g}, \theta) \propto p(\mathbf{g}|\mathbf{f}, \theta_\epsilon)\dot{p}(\mathbf{f}|\theta_f)$$
  where $\theta = (\theta_\epsilon, \theta_\mathbf{f})$ if θ is known (supervised case) or
  2. the joint a posteriori probability distribution
  $$p(\mathbf{g}, \theta|\mathbf{f}) \propto p(\mathbf{g}|\mathbf{f}, \theta_\epsilon)\dot{p}(\mathbf{f}|\theta_f)\dot{p}(\theta_\mathbf{f})\dot{p}(\theta_\epsilon)$$
  if θ is unknown (unsupervised case)
- Finally, based on these posterior probability laws, an estimator $\hat{f}$ for f and $\hat{\theta}$ for θ is defined.

The following section provides further details regarding the prior laws that need to be satisfied in order to derive the expressions of these posterior laws.

The Bayesian approach begins by making assumptions about ϵ from which the conditional probability laws can be deduced, i.e., $p(\mathbf{g}|\mathbf{f})$. For instance, if the maximum entropy (ME) principle is only known for the first two moments of ϵ, or if any other logical reasoning leads us to choose a Gaussian distribution. Let's assume that the variance is centered on ϵ, given by $p(\epsilon) = \mathcal{N}(0, \sigma_\epsilon^2\mathbf{I})$, where σ_ϵ^2 represents the variance, and $\mathbf{I}$ denotes the identity matrix.

$$\begin{aligned} p(\mathbf{g}|\mathbf{f}, \sigma_\epsilon^2) &= \mathcal{N}\big(\mathbf{H}(\mathbf{f}), \sigma_\epsilon^2\mathbf{I}\big) \\ &= \Big(\frac{1}{2\pi\sigma_\epsilon^2}\Big)^{\frac{M}{2}} \exp\Big\{\frac{-1}{2\sigma_\epsilon^2}\Big\|\mathbf{g} - \mathbf{H}(\mathbf{f})\Big\|^2\Big\} \end{aligned} \tag{3}$$

A priori model of the image pixels

In this paper, we make the assumption that the image $f(\mathbf{r})$ is composed of a finite set K of homogeneous regions R_k, where K is a known parameter (in the supervised case) with given labels $z(\mathbf{r}) = k$, where $k = 1, \ldots, K$. Each region R_k is defined as $R_k = \mathbf{r} : z(\mathbf{r}) = k$, and the entire image can be represented as the union of all these regions, denoted as $R = \cup_k R_k$. The pixel values corresponding to each region are represented as $\mathbf{f_k} = f(\mathbf{r}) : \mathbf{r} \in R_k$, and the entire image can be represented as $\mathbf{f_b} = \cup_k \mathbf{f_k}$.

The pixels in a given region are assumed to be independent and identically distributed (i.i.d.).

$$p\big(f(\mathbf{r})|z(\mathbf{r}) = k\big) = \mathcal{N}\big(f(\mathbf{r})|m_k, \sigma_k^2\big) \quad k = 1, \ldots K$$

and thus

$$\begin{aligned} p(\mathbf{f}|\mathbf{z}) &= \prod_{k=1}^{K} \mathcal{N}(m_k\mathbf{1}_k, \sigma_k^2\mathbf{I}_k) \\ &\propto \prod_{k=1}^{K} \exp\Big\{-\frac{1}{2\sigma_k^2}\Big\|\mathbf{f_k} - m_k\mathbf{1}_k\Big\|^2\Big\} \end{aligned} \tag{4}$$

A posteriori probability laws

To determine the posterior distributions, we need to apply Bayesian inference. By combining the prior distributions with the likelihood function, we can derive the posterior distributions. $p(\mathbf{f}|\mathbf{z}, \theta, \mathbf{g})$, $p(\theta|\mathbf{f}, \mathbf{z}, \mathbf{g})$ and $p(\mathbf{z}|\mathbf{f}, \theta, \mathbf{g})$ in order to sample these probabilities

- sampling $\mathbf{f}$ using $p\left(\mathbf{f}|\mathbf{z},\mathbf{g},\theta\right)$:

$$\begin{aligned} p\left(\mathbf{f}|\mathbf{z},\mathbf{g},\theta\right) &\propto p\left(\mathbf{g}|\mathbf{z},\mathbf{f},\theta\right)p\left(\mathbf{f}|\mathbf{z},\theta\right) \\ &\propto \mathcal{N}(\mathbf{g}|\mathbf{f},\sigma_\epsilon^2\,\mathbf{I})\prod_{k=1}^{K}p\left(f_k|z_k,\theta\right) \\ &\propto \mathcal{N}(\mathbf{g}|\mathbf{H}\,\mathbf{f},\sigma_\epsilon^2\,\mathbf{I})\prod_{k=1}^{K}p\left(f_k|m_k\mathbf{1},\sigma_k^2\mathbf{I}_k\right) \end{aligned} \tag{5}$$

- sampling $\mathbf{z}$ using $p(\mathbf{z}|\mathbf{f},\theta,\mathbf{g})$:

$$\begin{aligned} p(\mathbf{z}|\mathbf{f},\theta,\mathbf{g}) &\propto p(\mathbf{f}|\mathbf{z},\theta,\mathbf{g})\,p(\mathbf{z}|\theta,\mathbf{g}) \\ &= p(\mathbf{f}|\mathbf{z},\theta)\,p(\mathbf{z}|\theta) \\ &= p(\mathbf{z}).\prod_{\mathbf{r}\in\mathcal{R}}p(f(\mathbf{r})|z(\mathbf{r}),\theta) \end{aligned}$$

- sampling θ using $p(\theta|\mathbf{f},\mathbf{z},\mathbf{g})$

$$p(\theta|\mathbf{f},\mathbf{z},\mathbf{g}) \propto p(\mathbf{m},\sigma|\mathbf{f},\mathbf{z}).p(\sigma_\epsilon^2|\mathbf{g},\mathbf{f}) \tag{6}$$

$p(\mathbf{m},\sigma|\mathbf{f},\mathbf{z})$, $p(\mathbf{m},|\sigma,\mathbf{f},\mathbf{z})$ and $p(\sigma^2|\mathbf{m},\mathbf{f},\mathbf{z})$ are calculated using the priors fixed before :

Maximum a posteriori and QMCMC Gibbs sampling
Consider the maximum a posteriori (MAP) estimate, which is proposed as an approximation to obtain a sample from the distribution $p(\mathbf{f}|\mathbf{g},\mathbf{z},\theta)$. In our case, since $\mathbf{H}(\mathbf{f})$ is not a linear function of $\mathbf{f}$, it is not possible to obtain an exact sample from this distribution. Therefore, an approximation algorithm is proposed, which involves computing the maximum of the posterior distribution.

$$\begin{aligned} \hat{\mathbf{f}} &= arg\,max_{\,\mathbf{f}}\left\{p\left(\mathbf{f}|\mathbf{g},\theta,\mathbf{z}\right)\right\} \\ &= \arg\,min_{\,\mathbf{f}}\left\{J(\mathbf{f}|\mathbf{g},\theta,\mathbf{z})\right\} \end{aligned}$$

The Gibbs sampler is a Markov chain Monte Carlo (MCMC) algorithm used to approximate a sequence of observations from a specific multivariate probability distribution. It is particularly useful when direct sampling from the distribution is not feasible or computationally challenging. This sequence can be used to approximate the joint distribution to approximate the marginal distribution of one of the variables or some subset of the variables (for example the unknown parameters or latent variables); or to compute an integral (such as the expected value of one of the variables). Typically, some of the variables correspond to observations whose values are known and hence do not need to be sampled. Gibbs sampling is commonly used as a means of statistical inference especially Bayesian inference. It is a randomized algorithm that is an alternative to deterministic statistical inference method such as the Algorithm of expectation maximization (EM). Gibbs sampling like other QMCMC algorithms generates a Markov chain of samples each of which is correlated with surrounding samples.

1. **Previous work where the pixels are locally independent**

$$\hat{\mathbf{f}} = \arg\min_{\mathbf{f}}\left\{\frac{1}{2\sigma_\epsilon^2}\left\|\mathbf{g}-\mathbf{H}(\mathbf{f})\right\|^2 + \sum_{k=1}^{K}\sum_{\mathbf{r}\in R_k}\frac{1}{2\sigma_k^2}\left\|f(\mathbf{r})-m_k\right\|^2\right\} \tag{7}$$

2. The novelty of the algorithm lies in its ability to handle the case of locally dependent pixels. Unlike previous methods that assume local independence, this algorithm takes into account the dependencies between neighboring pixels.

$$\hat{\mathbf{f}} = \arg\min_{\mathbf{f}}\left\{\frac{1}{2\sigma_\epsilon^2}\left\|\mathbf{g}-\mathbf{H}(\mathbf{f})\right\|^2 - \sum_{k=1}^{K}\sum_{\mathbf{r}\in R_k}\frac{1}{\sigma_k^2}\left(\tilde{f}(\mathbf{r})-\beta_r\sum_{\mathbf{s}\in(\upsilon(\mathbf{r})\cap R_k)}\tilde{f}(\mathbf{s})\right)^2\right\} \tag{8}$$

where $\tilde{f}(\mathbf{r}) = f(\mathbf{r}) - m(\mathbf{r})$
β_r : coefficient depending on pixel $\mathbf{r}$ and equal to $\frac{1}{n_r}$ if $n_r \neq 0$ and equals to 0 otherwise
n_r : equal to card $\left(\nu(\mathbf{r})\cap R_k\right)$

Gibbs sampling

$$\begin{aligned} \hat{\mathbf{f}}^{(n+1)} = &\quad \arg\max_{\mathbf{f}}\{p(\mathbf{f}|\hat{z}^{(n)},\hat{\theta}^{(n)},\mathbf{g}\} \quad \text{for two cases} \\ \text{sample} &\quad \hat{\mathbf{z}}^{(n+1)} \sim p(\mathbf{z},|\hat{\mathbf{f}}^{(n)},\hat{\theta}^{(n)}) \\ \text{sample} &\quad \hat{\theta}^{(n+1)} \sim p(\theta,|\hat{\mathbf{f}}^{(n)},\hat{\mathbf{z}}^{(n)},\mathbf{g}) \end{aligned}$$

Given an initial state $(\hat{\theta},\hat{\mathbf{z}})^{(0)}$, the approximate Gibbs sampling method can be employed to estimate the collection of variables $(\mathbf{f},\mathbf{z},\theta)$.

The approximate Gibbs sampling method iteratively updates the variables by sampling from their conditional distributions, assuming the other variables are fixed. The algorithm proceeds as follows:

Set the iteration counter t to 0 and initialize the variables $(\hat{\theta},\hat{\mathbf{z}})$ as $(\hat{\theta},\hat{\mathbf{z}})^{(0)}$.

Repeat the following steps until convergence or a predefined number of iterations: a. Increment the iteration counter: $t \leftarrow t+1$. b. Sample the variable $\mathbf{f}$ from its conditional distribution given the current values of $(\hat{\theta},\hat{\mathbf{z}})$. c. Sample the variable $\mathbf{z}$ from its conditional distribution given the current values of $(\hat{\theta},\hat{\mathbf{f}})$. d. Sample the variable θ from its conditional distribution given the current values of $(\hat{\mathbf{f}},\hat{\mathbf{z}})$.

Output the estimated values of $(\mathbf{f},\mathbf{z},\theta)$ after convergence or the desired number of iterations.

It's important to note that in approximate Gibbs sampling, the conditional distributions can be approximated using various techniques, such as mean field approximation or variational inference, depending on the complexity of the model and the desired computational efficiency.

The approximate Gibbs sampling method allows for the estimation of the variables $(\mathbf{f},\mathbf{z},\theta)$ by iteratively sampling from their conditional distributions, incorporating the dependencies and relationships among the variables. This approach is commonly used in Bayesian inference and can be

applied to various problems in statistics and machine learning.

Simulation results

The numerical phantom model used for these simulations consists of an air-filled cuboid measuring 300 $\times$ 300 $\times$ 256. The cuboid contains a central cylinder that serves as the background material. Within the central cylinder, smaller cylinders made of different materials are embedded at a fixed distance from the origin. A schematic representation of the phantom and the corresponding materials is shown in Fig.1a. The image is reconstructed from its noisy spectral modulus in the Fourier domain. The parameters and hyperparameter values are chosen as follows: the PMRF parameter, denoted as α, is set to 2, and the image's class number, represented by K, is equal to 4.

In our approach, the original image $\mathbf{f}$ has been normalized to a range between 0 and 1. For all k, the following parameters are chosen: $m_0 = 0$, $\sigma_0^2 = 1$, $\alpha_0 = 2$, $\beta_0 = 1$, $\alpha_0^\epsilon = 2$, and $\beta_0^\epsilon = 1$.

We utilize the Potts-Markov model in our strategy for label assignment, as it represents both the Gaussian independent model (IGM) and the Gauss-Markov random field model (GMRF) for pixels (Eq. 8). To optimize computational efficiency and achieve superior results, we apply a Markov chain quasi-Monte Carlo (QMCMC) technique, specifically the Maximum a Posteriori Probability (MAP) Gibbs sampling method. Since the object consists of homogeneous regions, the histogram serves as a useful tool to showcase the effectiveness of the reconstruction. Each peak in the histogram corresponds to a different region of the object being reconstructed. The accuracy of the reconstruction is assessed by examining each peak, which represents a separate material within the object. As the number of iterations increases, the image reconstruction using spectral magnitude approaches near-perfection. Figure 4 presents the observed magnitude over the frequency range, the correlation between the original and reconstructed image, and the correlation plotted versus the signal-to-noise ratio.

Comparative study

0.1 Comparison to some deterministic methods

A comparative analysis has been conducted between our technique and other algorithms, namely [5], [7], and [8], in order to assess the effectiveness of our algorithm. Visually, as depicted in Figure 4, the reconstruction quality achieved by our technique is satisfactory.

However, when comparing our technique to [5] and [7], it is observed that these algorithms diverge and produce unrecognizable images. On the other hand, [8] exhibits convergence to an acceptable, though not superior, quality in the reconstruction process.

This comparative analysis highlights the superiority of our technique in terms of reconstruction quality when compared to the aforementioned algorithms. The visually satisfactory results obtained with our technique further support its effectiveness in image reconstruction.

0.2 The robustnbess of Gauss-Markov Prior

The Gauss-Markov prior exhibits robustness in the context of image reconstruction. By incorporating this prior into the reconstruction process, it helps to capture the underlying statistical properties of the image.

The Gauss-Markov prior assumes that neighboring pixels in the image exhibit a certain level of correlation or similarity. This prior knowledge is leveraged to regularize the reconstruction and encourage smoothness in the estimated image. As a result, the Gauss-Markov prior helps to reduce noise, artifacts, and inconsistencies in the reconstructed image.

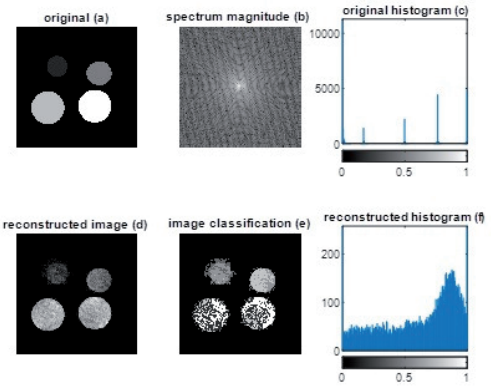

(a) The joint image classification and reconstruction process is performed using magnitude-only information for a total of 100 iterations.

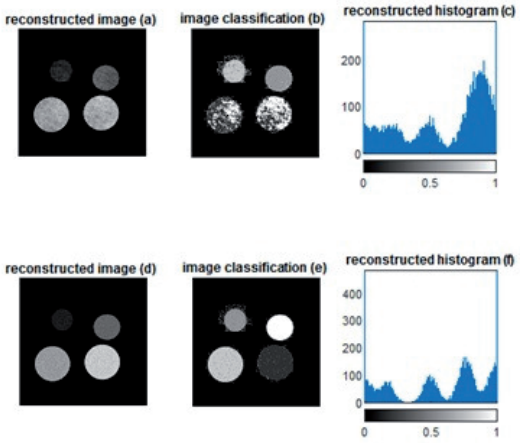

(b) The joint image classification and reconstruction process is performed using magnitude-only information for 200 and 300 iterations, respectively.

Fig. 2: The joint image classification and reconstruction process is performed using only magnitude information.

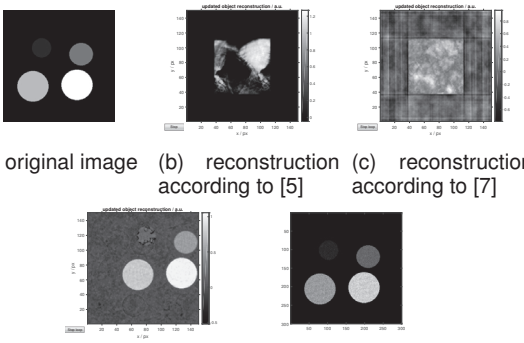

(a) original image (b) reconstruction according to [5] (c) reconstruction according to [7]

(d) reconstruction according to [8] (e) reconstruction using the proposed approach

Fig. 3: Comparison of magnitude only based image reconstruction

(a) Spectral magnitude mask

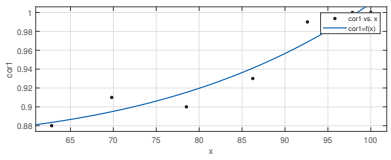

(b) Correlation vs spectral magnitude quantity

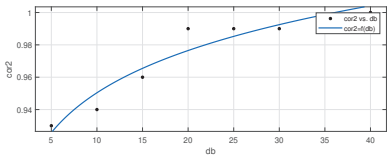

(c) Correlation coefficient vs Signal to Noise Ration (dB)

Fig. 4: Performance of image reconstruction approach

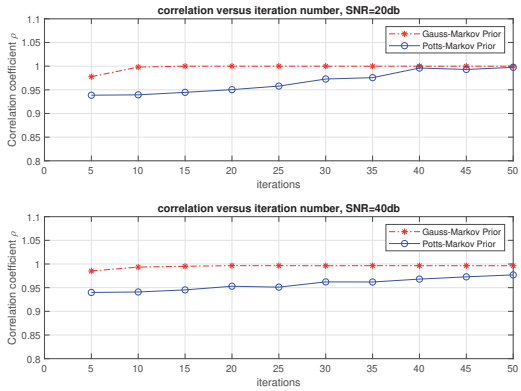

(a) Correlation coefficient vs iteration number with Potts-Gauss-Markov Prior

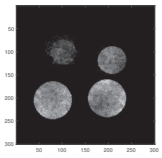

(b) Image reconstruction with Potts-Markov Prior, (5 iterations)

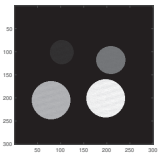

(c) Image reconstruction with Gauss-Markov Prior, (5 iterations)

Fig. 5: Performance of image reconstruction approach with Gauss-Markov Prior

Conclusion

The reconstructed images are displayed under a corrupted observation noise with a signal-to-noise ratio (SNR) of 20 dB and a fixed number of iterations. The results clearly demonstrate that approximately 100 iterations are required to achieve a flawless reconstruction of the pixels, utilizing the Gauss-Markov Random Field model, while preserving the edges of each region. The inclusion of local dependent pixel information within each zone significantly improves the algorithm's performance, even in the presence of noise. This joint reconstruction and classification method has effectively demonstrated its efficacy for images with homogeneous regions. One of the key advantages of the Gauss-Markov prior is its ability to handle various noise models. It is robust against different types of noise, such as Gaussian noise, Poisson noise, or even more complex noise models. This is particularly important in real-world scenarios where the presence of noise is inevitable. Additionally, the Gauss-Markov prior provides a flexible framework that can be adapted to different imaging scenarios. It can be combined with other priors or constraints to further improve the reconstruction quality, depending on the specific application requirements.

Acknowledgment

We would like to express our sincere gratitude to Dr. Tatiana Latychevskaia from the Paul Scherrer Institute, Switzerland. Her generous contribution of the Matlab code was instrumental in conducting the comparison study and completing the work presented in this article. We greatly appreciate the valuable support of Pr. A.M. Djafari, CNRS for which significantly enhanced the quality and depth of our research.

***Authors**: Ph.D. student, Bagdaoui Amina, Ph.D. Bendaoudi Amina. Faculty of Electrical Engineering. LEPO Laboratory. Djillali Liabes University in Sidi Bel Abbes, BP. 89. Algeria. email: bagdaoui.amina@outlook.fr. Prof. A. Djafari, CNRS, Research center. France.*

REFERENCES

[1] Patterson, A. L.(1934). A Fourier series method for the determination of the components of interatomic distances in crystals.*Physical Review. 46*, 5, 372.

[2] Patterson, A. L.(1944). Ambiguities in the X-ray analysis of crystal structures, *Physical Review. 46*, 5, 372.

[3] Romain Arnal.(2019). Aspects of Phase Retrieval in X-ray Crystallography, *Thesis*, University of Canterbury, Christchurch, New Zealand.

[4] J. C. Dainty and J. R. Fienup.(1987). Phase retrieval and image reconstruction for astronomy, *Image Recovery: Theory and Application*: 231-275.

[5] J. R. Fienup.(1982). Phase retrieval algorithms: a comparison, *Applied Optics*: 21(15), 2758-2769.

[6] Tatiana Latychevskaia.(2018). Iterative phase retrieval in coherent diffractive imaging: practical issues, *Applied Optics* 57(25), 7187 - 7197 (2018)

[7] J. Miao et al.(1998) Phase retrieval from the magnitude of the Fourier transforms of nonperiodic objects, *J. Opt. Soc. Am. A*, 15(6), 1662 - 1669 (1998)

[8] S. Marchesisni et al.(2003) X-ray image reconstruction from a diffraction pattern alone, *Phys. Rev. B* 68(14), pages 140101 (2003)

[9] Shiro Ikeda and Hidetoshi Kono.(2012). Phase retrieval from single biomolecule diffraction pattern, *Optic express*, 20, 4: 3375-3387.

[10] L. Rabiner and B. H. Juang.(1993). Fundamentals of speech recognition, *Prentice Hall*.

[11] A. Walther.(1963). The question of phase retrieval in optics, *Journal of Modern Optics. 10*, 1,: 41-49.

[12] Y. Shechtman; Yonina C. Eldar; Oren Cohen; H. N. Chapman; J. Miao; M. Segev.(2015). Phase Retrieval with Application to Optical Imaging: A contemporary overview, *IEEE Signal Processing Magazine*, 32, 3: 87-109.

[13] R. P. Millane.(1990) Phase retrieval in crystallography and optics, *JOSA A, 7*, 3: 394-411.

[14] A. Orlowski, H. Paul.(1994). Phase retrieval in quantum mechanics, *Physical review A, Atomic, molecular, and optical physics*, 50, 2: 921-924.

[15] R. W. Gerchberg, W. O. Saxton.(1972). A practical algorithm for the determination of the phase from image and diffraction plane pictures, *Optik*, 35, 237.

[16] Praneeth Netrapalli, Prateek P JainPrateek P Jain, Sujay Sanghavi.(2013). Phase Retrieval Using Alternating Minimization, *IEEE Transactions on Signal Processing*, 63, 18.

[17] Hui-ping Li, Song Li.(2020). Phase retrieval with PhaseLift algorithm, *Applied Mathematics*, 35, 4: 479-502

[18] Emmanuel Candes, Xiaodong Li, Mahdi Soltanolkotabi.(2015) Phase Retrieval via Wirtinger Flow: Theory and Algorithms, *IEEE Transactions on Information Theory*, 64, 4: 1985-2007

[19] Jian-Wei, LiuZhi-Juan, CaoJing LiuShow, Long-Chuan Guo.(2019) Phase Retrieval via Wirtinger Flow Algorithm and Its Variants, *Conference: 2019 International Conference on Machine Learning and Cybernetics (ICMLC)*, July 2019
[20] Tom Goldstein, Christoph Studer.(2018) PhaseMax: Convex Phase Retrieval via Basis Pursuit, *IEEE Transactions on Information Theory*, 64, 4: 2675-2689
[21] Ming-Hsun Yang, Y.-W. Peter Hong, Jwo-Yuh Wu.(2021) Sparse Affine Sampling: Ambiguity-Free and Efficient Sparse Phase Retrieval, *IEEE Transactions on Information Theory (Early Access)*, 21 June 2022, Page(s): 1-1
[22] Namrata Vaswan, Seyedehsara Nayer, Yonina C. Eldar.(2017) Low-Rank Phase Retrieval, *IEEE Transactions on Signal Processing*, 65, 15, 4059-4074
[23] Jeffrey W. Miller, Matthew T. Harrison.(2017) Mixture Models With a Prior on the Number of Components, *Journal of the American Statistical Association*, 113, 521: 340-356
[24] Eugene A. Opoku, Syed Ejaz Ahmed, Trisalyn Nelson, Farouk S. Nathoo.(2020) Parameter and Mixture Component Estimation in Spatial Hidden Markov Models: A Comparative Analysis of Computational Methods, *Proceedings of the Fourteenth International Conference on Management Science and Engineering Management. ICMSEM 2020. Advances in Intelligent Systems and Computing*, vol 1190. Springer
[25] Redha Touati, Max Mignotte, Mohamed Dahmane.(2019) Multimodal Change Detection in Remote Sensing Images Using an Unsupervised Pixel Pairwise-Based Markov Random Field Model, *IEEE Transactions on Image Processing*, 29: 757-767